Establishing a Blueprint for CED-3-dependent Killing through Identification of Multiple Substrates for This Protease*⒮

Rebecca C. Taylor[‡], **Gabriela Brumatti**[‡], **Shu Ito**[§], **Michael O. Hengartner**[¶], **W. Brent Derry**[§], and **Seamus J. Martin**[‡1]

From the [‡]*Molecular Cell Biology Laboratory, The Smurfit Institute of Genetics, Trinity College, Dublin 2, Ireland, the* [§]*Program in Developmental Biology, Hospital for Sick Children & Department of Medical and Molecular Genetics, University of Toronto, Ontario M5G 1X8, Canada, and the* [¶]*Institute of Molecular Biology, University of Zurich, Winterthurerstrasse 190, CH-8057 Zurich, Switzerland*

Genetic studies have established that the cysteine protease CED-3 plays a central role in coordinating programmed cell death in *Caenorhabditis elegans*. However, it remains unclear how CED-3 activation results in cell death because few substrates for this protease have been described. We have used a global proteomics approach to seek substrates for CED-3 and have identified 22 worm proteins that undergo CED-3-dependent proteolysis. Proteins that were found to be substrates for CED-3 included the cytoskeleton proteins actin, myosin light chain, and tubulin, as well as proteins involved in ATP synthesis, cellular metabolism, and chaperone function. We estimate that ~3% of the *C. elegans* proteome is susceptible to CED-3-dependent proteolysis. Notably, the endoplasmic reticulum chaperone calreticulin, which has been implicated in the recognition of apoptotic cells by phagocytes, was cleaved by CED-3 and was also cleaved by human caspases during apoptosis. Inhibitors of caspase activity blocked the appearance of calreticulin on the surface of apoptotic cells, suggesting a mechanism for the surface display of calreticulin during apoptosis. Further analysis of these substrates is likely to yield important insights into the mechanism of killing by CED-3 and its human caspase counterparts.

The caspase family of cysteine proteases have been implicated in the regulation of programmed cell death in numerous organisms, from simple invertebrates to man (1). Caspases are present in most cells as inactive proenzymes and become activated during apoptosis through diverse signaling pathways (2, 3). Upon activation, caspases promote programmed cell death by restricted proteolysis of numerous proteins within the dying cell (4). Caspase-dependent proteolytic events produce dramatic rearrangements of the cellular architecture and engulfment of the dying cell by phagocytes (5).

The nematode *Caenorhabditis elegans* has contributed greatly to our understanding of the regulation of cell death in metazoans through discovery of a series of cell death defective (ced) genes (6, 7). In several cases, this led directly to the discovery of a role for their mammalian counterparts in the regulation of apoptosis, the caspases being a notable example (8–10). The worm caspase, CED-3, has been established as essential for the great majority of developmentally related programmed cell deaths in the worm (6, 11). Similar to mammalian caspases, CED-3 is probably present in most cells as an inactive precursor but becomes activated in cells fated to die during development. CED-3 activation is achieved through recruitment of the inactive CED-3 precursor to the scaffold protein CED-4, which assembles into a tetrameric complex (12). The latter event is normally prevented by CED-9, which represses CED-4 tetramerization and CED-3 recruitment (12, 13). However, although CED-3 is firmly established as a central participant in the molecular control of programmed cell death in the worm, how activation of this protease results in cell death is obscure because few substrates for CED-3 have been identified thus far. Understanding how CED-3 kills cells in the worm is of considerable interest, not only because this is likely to shed further light upon how programmed cell death is coordinated in this organism, but because this is also likely to generate insight into how human caspases promote apoptosis. The observation that a single caspase is sufficient to coordinate apoptosis in the worm suggests that CED-3 harbors all of the activities that have subsequently become allocated to several different caspases in higher organisms.

Here we have used two-dimensional gel-based proteomics to seek substrates for CED-3. This approach yielded 22 substrates and included proteins involved in protein and DNA synthesis, chaperone function, cellular metabolism, and the cytoskeleton. We estimate that ~3% of the worm proteome is susceptible to CED-3-dependent proteolysis. These data suggest that CED-3 promotes cell death through simultaneously targeting diverse cellular functions. Detailed analysis of these substrates is likely to yield important insights into the mechanism of killing by CED-3.
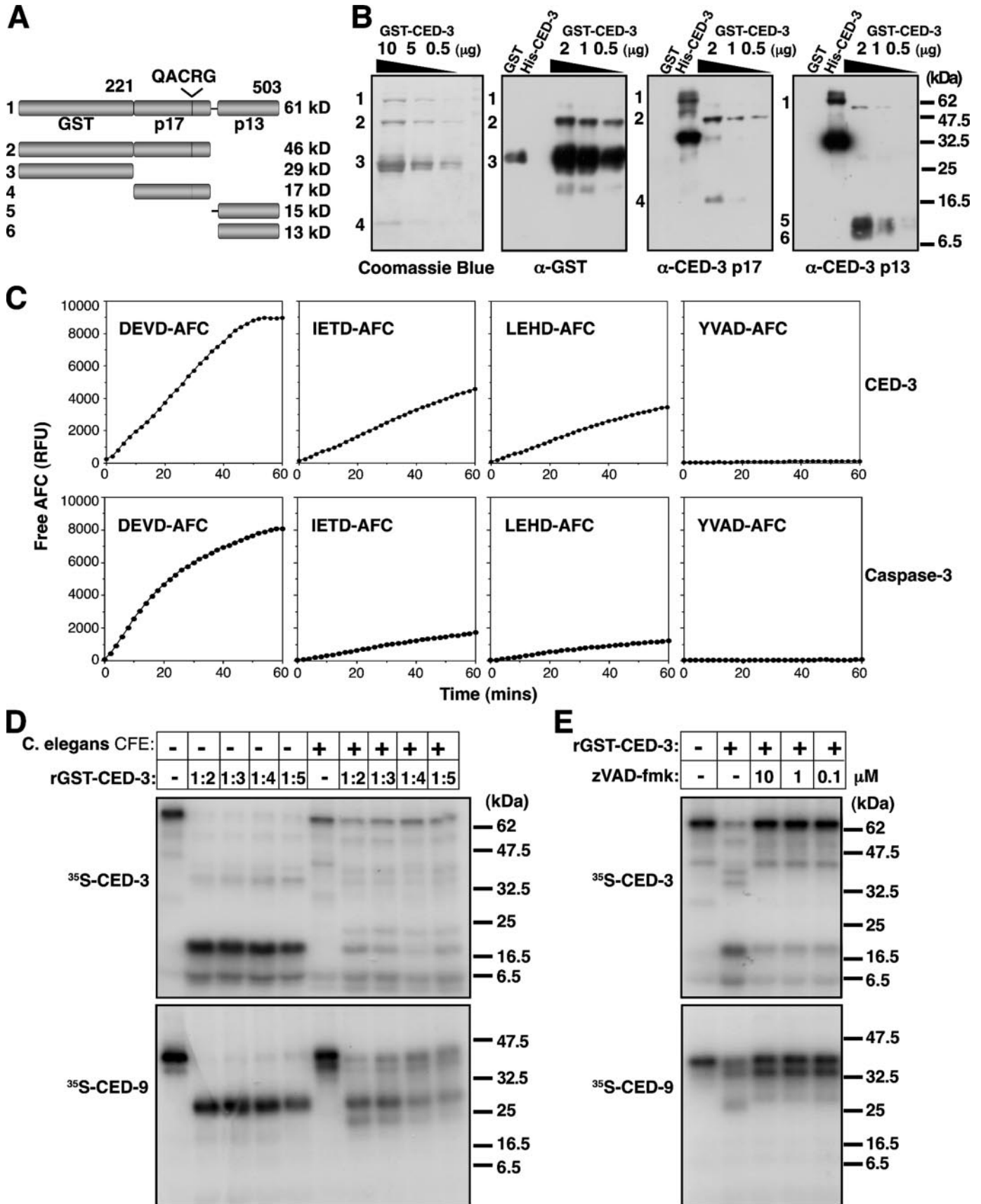
EXPERIMENTAL PROCEDURES

Reagents—The following antibodies were used for immunoblotting: anti-CED-3 C-20 (Santa Cruz), anti-GST (BD Pharmingen), anti-β-tubulin (ICN), anti-calreticulin polyclonal antibody (Affinity Bioreagents), and anti-calreticulin monoclonal antibody (Transduction Laboratories). Anti-calreticulin polyclonal antibody was also used for surface immunostaining in conjunction with anti-rabbit Alexafluor 488 as a secondary

antibody (Molecular Probes). Rabbit polyclonal antibodies were generated against recombinant CED-3, as follows. Briefly, His-CED-3[221–503] was expressed in *Escherichia coli* and purified over nickel-nitrilotriacetic acid-agarose, and rabbits were immunized with the purified protein. Polyclonal antibodies against p17 and p13 domain peptides of CED-3 were also generated and affinity-purified using the immunization peptides. The peptides z-VAD-fmk,[2] Ac-DEVD-AFC, Ac-LEHD-AFC, Ac-IETD-AFC, and Ac-YVAD-AFC were purchased from Bachem. 17-cm immobilized pH gradient strips (pH 3–6 and pH 5–8), easy melt agarose and Bio-Lyte ampholytes[TM] were obtained from Bio-Rad. The serine protease inhibitors, tosyl-phenylalanylchloromethane, and 3,4-dichloroisocoumarin (DCI) were purchased from Merck. Unless otherwise indicated, all other reagents were purchased from Sigma.

Plasmids and Site-directed Mutagenesis—The CED-3[221–503] open reading frame was cloned from a pQE30-CED-3[221–503] template (kindly provided by Dr. Shai Shaham) into the pGEX4TK2 vector to generate GST-tagged CED-33[221–503]. Crt-1, Tbb-2, and Ftt-2 open reading frames were amplified by PCR from a *C. elegans* cDNA library (Origene) and cloned into the pET45b vector. The human calreticulin open reading frame was amplified by PCR from an IMAGE clone (MRC) and inserted into pcDNA3. Site-directed mutagenesis was carried out using a QuikChange kit (Stratagene). All of the plasmids were verified by DNA sequencing.

Expression and Purification of Recombinant CED-3—*E. coli* DH5α cells were transformed with pGEX4TK2-CED-3[221–503]. CED-3 protein expression was induced by the addition of 100 μM isopropyl β-D-thiogalactopyranoside to culture medium followed by a 3-h incubation at 25 °C. Proteins were affinity-purified on glutathione-Sepharose, as previously described, and eluted in protease reaction buffer (50 mM HEPES, pH 7.4, 75 mM NaC1, 0.1% CHAPS, 2 mM dithiothreitol) with 10 mM glutathione. CED-3 was then active site titrated against Ac-DEVD-AFC, using z-VAD-fmk as an inhibitor.

Fluorimetry Assays—The Reactions containing recombinant GST-CED-3[221–503] were typically assembled in a final volume of 100 μl, containing 50 μM Ac-DEVD-AFC, Ac-LEHD-AFC, Ac-IETD-AFC, or Ac-YVAD-AFC in protease reaction buffer. Fluorescence was then measured in an automated fluorimeter (Spectrafluor Plus; TECAN) at wavelengths of 430 nm (excitation) and 535 nm (emission).

---

[2] The abbreviations used are: z, benzyloxycarbonyl; fmk, fluoromethyl ketone; DCI, 3,4-dichloroisocoumarin; GST, glutathione *S*-transferase; CHAPS, 3-[(3-cholamidopropyl)dimethylammonio]-1-propanesulfonic acid; MALDI-TOF, matrix-assisted laser desorption ionization time-of-flight; FACS, fluorescence-activated cell sorter.

Coupled in Vitro Transcription/Translation—[35S]Methionine-labeled proteins were generated using the TNT kit (Promega) as described previously (35). Typically, 25-μl reactions were assembled containing 0.5 μg of template plasmid DNA and 2 μl of translation grade [35S]methionine (1000 μCi/ml; MP Biomedicals).

Nematode Cell-free Reactions—Bristol N2 strain *C. elegans* were harvested from a 250-ml liquid culture by centrifugation at 500 × *g* for 5 min. Nematodes were washed twice in 50 ml of 100 mM NaCl, added to 20 ml of 60% sucrose, and centrifuged for 5 min at 5000 × *g*. Worms were immediately removed from the sucrose and washed in 100 mM NaCl. Following a final centrifugation at 500 × *g*, pelleted worms were resuspended in 2 volumes of extract buffer (20 mM HEPES-KOH, pH 7.5, 10 mM KCl, 1.5 mM MgCl$_2$, 1 mM EDTA, 1 mM EGTA, 1 mM dithiothreitol, 100 μM phenylmethylsulfonyl fluoride, 10 μg/ml leupeptin, 2 μg/ml aprotonin). Resuspended worms were lysed by sonication, and insoluble material was pelleted for 15 min at 15,000 × *g*. CED-3 was added to soluble *C. elegans* extract at 130 nM (as determined by active site titration with z-VAD-fmk) unless otherwise indicated. The reactions were incubated for 2 h at 37 °C to facilitate CED-3-dependent proteolysis. Cell-free reactions were then assessed by immunoblotting or subjected to two-dimensional electrophoresis as described.

Two-dimensional Electrophoresis—Approximately 500 μg of protein was solubilized to a final volume of 350 μl in IEF sample buffer (8 M urea, 4% CHAPS, 0.05% SDS, 100 mM dithiothreitol, 0.2% w/v Bio-Lyte ampholytes[TM], 0.02% (w/v) bromphenol blue). Immobilized pH gradient strips were passively rehydrated in the presence of protein samples overnight. The samples were then focused on a Bio-Rad IEF cell under the following conditions: 1) a linear voltage ramp to 500 V over 1 h, 2) 5 h at a constant 500 V to facilitate desalting, 3) linear voltage ramp to 3500V over 5 h, and 4) 15 h at a constant 3500 V. Following isoelectric focusing, immobilized pH gradient strips were prepared for second dimension SDS-PAGE by a 10-min incubation in reducing buffer (2% (w/v) dithiothreitol in 6 M urea, 375 mM Tris-HCl, pH 8.8, 2% SDS, 20% glycerol), followed by a 10-min incubation in alkylating buffer (2.5% (w/v) iodoacetimide in 6 M urea, 375 mM Tris-HCl, pH 8.8, 2% SDS, 20% glycerol). Strips were then mounted on 12% SDS-PAGE gels using 1–2 ml of easy melt agarose (Bio-Rad) and electrophoresed at 37.5 mA/gel in a Bio-Rad Protean IIxi electrophoresis cell (Bio-Rad).

Silver Staining of Two-dimensional Gels—Proteins were visualized using a mass spectrometry-compatible silver staining protocol as previously described (14). Silver-stained gel images were acquired using a digital camera and were visually inspected for CED-3-dependent changes in spot patterns.

FIGURE 1. **Proteolytic activity of purified GST-CED-3.** *A*, schematic showing predicted products of GST-CED-3[221–503] autoproteolysis. *B*, GST-tagged CED-3[221–503] was expressed in *E. coli* and purified from bacterial lysates. Purified protein was electrophoresed through 12% SDS-PAGE gels and either stained with Coomassie Blue or subjected to Western blotting with antibodies specific to GST and the p17 and p13 subunits of CED-3. Purified GST alone and purified recombinant His[6]-tagged CED-3[221–503] were also loaded as controls. The bands are labeled according to the scheme shown in *A*. *C*, purified GST-CED-3[221–503] and human caspase-3 were assayed for their ability to support hydrolysis of the fluorogenic caspase substrate peptides ac-DEVD-AFC, ac-IETD-AFC, ac-LEHD-AFC, and ac-YVAD-AFC. *D*, a range of concentrations of GST-CED-3[221–503] were added to [35S]Met-labeled CED-3 and CED-9 with or without *C. elegans* mixed stage cell-free extract (*CFE*). Ratios shown represent dilutions of the CED-3 protease stock. The stock concentration of CED-3 was 400 nM; therefore, the concentrations used were 200, 130, 100, and 80 nM. The reactions were incubated for 2 h at 37 °C followed by electrophoresis on 12% SDS-PAGE gels. *E*, [35S]Met-labeled CED-3 and CED-9 were incubated for 2 h at 37 °C with 100 nM of GST-CED-3[221–503] and a range of concentrations of the caspase inhibitor z-VAD-fmk, followed by electrophoresis on 12% SDS-PAGE gels.
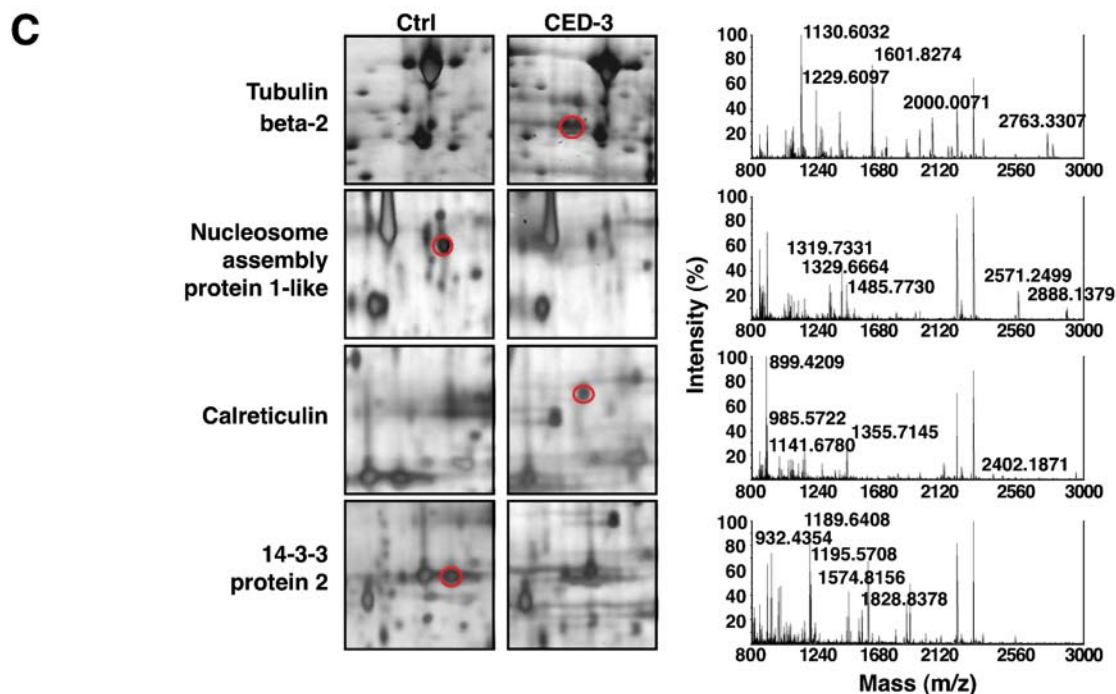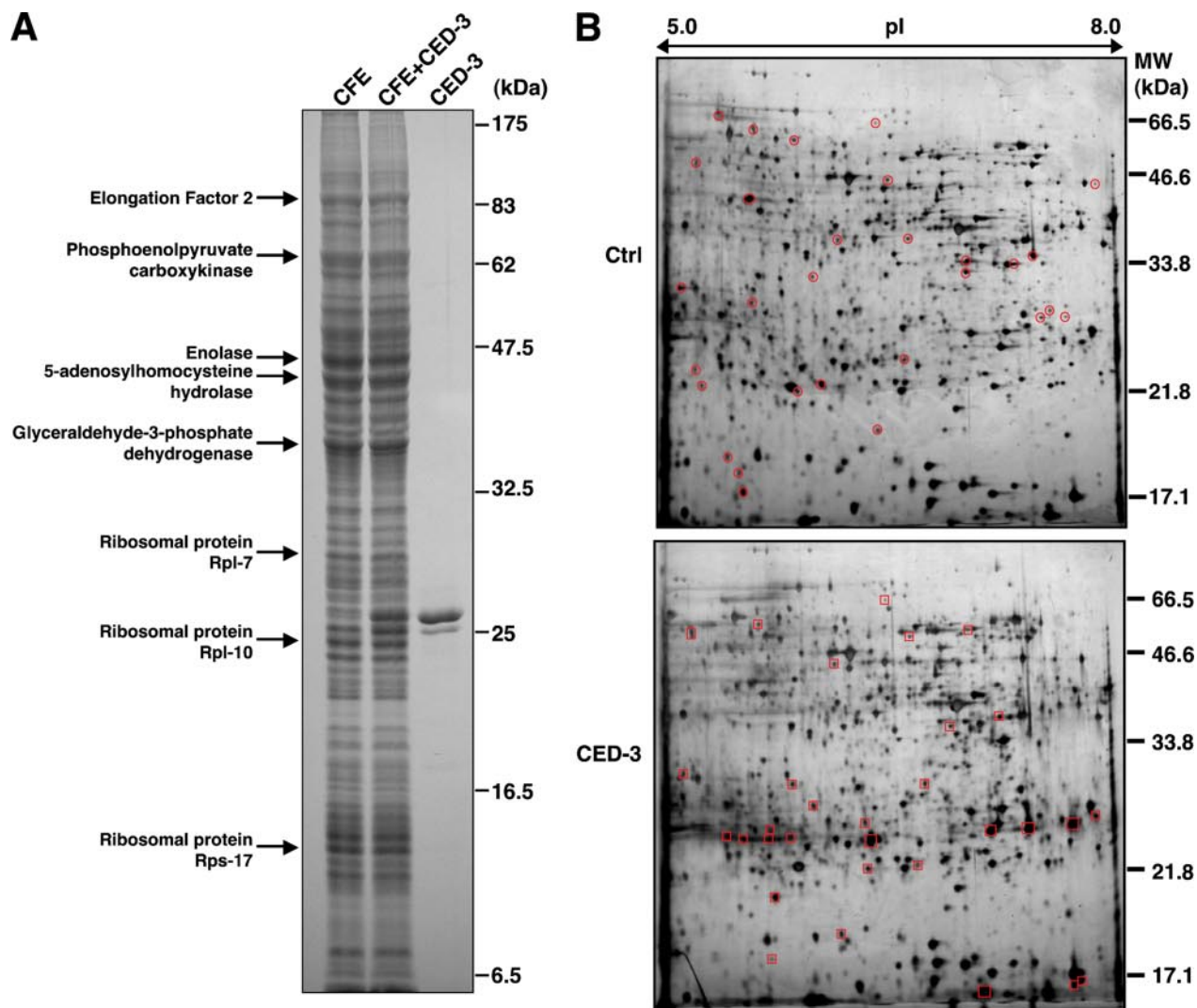
In-gel Protein Digestion and Identification by MALDI-TOF Mass Spectrometry—Candidate protein spots were excised from two-dimensional gels, in-gel digested with trypsin, extracted, and identified by MALDI-TOF mass spectrometry (ABI Voyager DE-Pro), as previously described (14).

Cell Culture and Induction of Apoptosis—CEM cells were cultured in RPMI 1640, 10% fetal calf serum under standard conditions. Apoptosis was induced by incubation in indicated concentrations of actinomycin D, tosylphenylalanylchloromethane, or DCI. To quantitate apoptosis, the cells were stained with annexin V-fluorescein isothiocyanate at 1 µg/ml and propidium iodide at 10 µg/ml in annexin V binding buffer (10 mM HEPES-NaOH, pH 7.4, 150 mM NaCl, 5 mM KCl, 1 mM MgCl$_2$, 1.8 mM CaCl$_2$). Cell fluorescence was measured on a flow cytometer (FACSCalibur, Becton Dickinson, CA).

Immunostaining—The cells were washed with phosphate-buffered saline containing 3% bovine serum albumin and 0.05% NaN$_3$, followed by a 15-min incubation in the same buffer. Antibodies were added at 1:400 and incubated for 1 h. After a further three washes, secondary antibody was added at 1:500 for 1 h. The cells were washed another three times and fixed for 15 min in phosphate-buffered saline with 3% paraformaldehyde and then prepared for flow cytometry.

Preparation of Cell Lysates—The cells were pelleted at 800 × g and resuspended at 2×10^7 cells/ml in SDS-PAGE loading buffer (2% SDS, 50 mM Tris-HCl, pH 6.8, 10% glycerol, 2.5% β-mercaptoethanol). The lysates were assessed by immunoblotting.

Preparation and Activation of Jurkat Cell-free Extracts—Cell-free extracts were prepared from human Jurkat cells, and caspases were activated by the addition of cytochrome *c* and dATP to these extracts, as described previously (14, 15).

RESULTS

CED-3 Displays Characteristics of Initiator and Effector Caspases—Programmed cell death in the nematode takes place in scattered cells during development such that of a total of 1090 cells born in the *C. elegans* hermaphrodite, 131 of these die in a programmed manner (16). Preliminary studies established that it was not possible to induce coordinate programmed cell death in worm embryos or in the somatic cells of adult worms using UV radiation, microtubule-disrupting drugs, or inhibitors of protein or RNA synthesis.[3] The latter stimuli readily trigger apoptosis in fly and mammalian cells, and their failure to do so in the worm suggests that a damage-associated programmed cell death pathway is absent in the majority of somatic cells in the nematode. Because it was not possible to

---

[3] R. C. Taylor and S. J. Martin, unpublished data.

obtain homogenous populations of dying cells from worm embryos or larval stages, we adopted a biochemical approach to finding CED-3 substrates. This involved generating homogenates from mixed stage worm populations, to which recombinant active CED-3 was added.

To obtain recombinant CED-3 we generated a variety of expression constructs including full-length CED-3, a truncated CED-3 lacking the N-terminal prodomain, and constructs encoding the large and small subunits individually. However, most of these failed to produce soluble protein, and several denaturation and refolding strategies proved unsuccessful (data not shown). Recombinant active CED-3 was produced by removing the N-terminal CARD domain of the protease (amino acids 1–220) and replacing with GST (Fig. 1, *A* and *B*). Purified GST-CED-3 fusion protein exhibited robust proteolytic activity against several synthetic caspase substrate peptides including DEVD-AFC, IETD-AFC, and LEHD-AFC (Fig. 1*C*). In contrast, CED-3 did not hydrolyze YVAD-AFC, a substrate that is commonly preferred by inflammatory caspases in mammals. CED-3 exhibited a preference for DEVD-AFC, which is typical of mammalian effector caspases such as caspase-3, but was also capable of cleaving IETD-AFC and LEHD-AFC relatively efficiently (Fig. 1*C*). Importantly, an N-terminally His-tagged CED-3 construct also displayed similar activity toward tetrapeptide substrates (supplemental Fig. S1), suggesting that the addition of the N-terminal GST moiety did not significantly alter the specificity of CED-3 toward peptide substrates. Thus, CED-3 appears to be more promiscuous than the major effector caspase in mammals (caspase-3), which is consistent with the role of CED-3 as the only essential effector, as well as initiator, caspase in the worm.

We also assessed the catalytic activity of recombinant CED-3 using protein substrates that were produced by coupled *in vitro* transcription/translation. CED-3 has previously been reported to cleave its own precursor, consistent with its ability to autoactivate (17). Moreover, CED-3 is also reported to cleave the cell death inhibitor CED-9 *in vitro* (18). Therefore, we titrated recombinant GST-CED-3 onto ^{35}S-labeled pro-CED-3 and ^{35}S-labeled CED-9 to assess the ability of CED-3 to cleave these proteins (Fig. 1*D*). As Fig. 1*D* illustrates, CED-3 cleaved its own precursor to fragments of ~17 and ~13 kDa consistent with separation of the large and small subunits through proteolysis at Asp[374] and Asp[388]. However, the addition of *C. elegans* homogenate (see below) significantly attenuated the activity of GST-CED-3 toward both ^{35}S-labeled substrates (Fig. 1*D* and supplemental Fig. S2). CED-3-mediated proteolysis of pro-CED-3 and CED-9 was also largely suppressed by the polycaspase inhibitor z-VAD-fmk (Fig. 1*E*).

FIGURE 2. **Detection of CED-3-induced alterations in the *C. elegans* proteome.** *A*, homogenates of mixed stage *C. elegans* populations (*CFE*) were treated with recombinant GST-CED-3 (final concentration, 130 nM) for 2 h at 37 °C. CED-3-treated homogenates were electrophoresed alongside mock treated lysates on one-dimensional 12% SDS-PAGE gels. An equivalent amount of CED-3 alone (*i.e.* without *C. elegans* cell-free extract) was also loaded for comparison. The proteins were visualized by staining with Coomassie Blue. The indicated proteins (*arrows*) represent abundant landmark proteins that were identified by MALDI-TOF mass spectrometry. *B*, protein samples (450 µg) from *C. elegans* homogenates mock treated or incubated with CED-3 (final concentration, 130 nM) as above were subjected to isoelectric focusing on pI 5–8 immobilized pH gradient strips followed by electrophoresis through 12% second-dimension SDS-PAGE gels. The proteins were visualized by silver staining. Protein spots disappearing upon treatment with CED-3 are *circled*; those appearing after CED-3 treatment are enclosed by *squares*. *C*, enlarged regions of two-dimensional SDS-PAGE gels are shown. Proteins reproducibly altered upon CED-3 treatment, either disappearing or appearing upon treatment of homogenates with CED-3, are indicated by *circles*. The MALDI-TOF mass spectrograms used to identify these proteins are shown alongside. Other protein changes occurring in these panels are additional CED-3-mediated alterations that have not been annotated here to focus upon individual changes. *MW*, molecular mass; *Ctrl*, control.
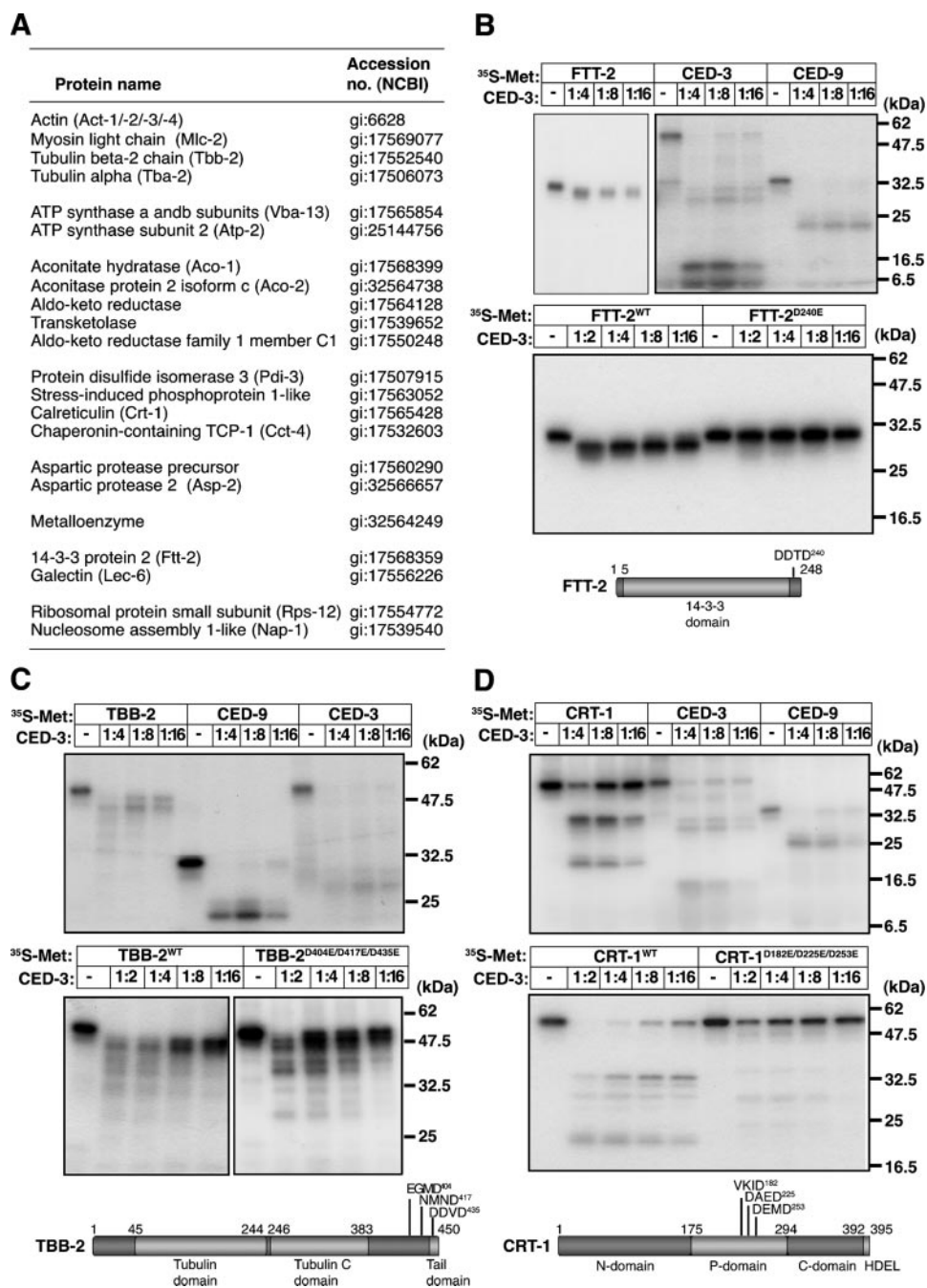
A

Protein name	Accession no. (NCBI)
Actin (Act-1/-2/-3/-4)	gi:6628
Myosin light chain (Mlc-2)	gi:17569077
Tubulin beta-2 chain (Tbb-2)	gi:17552540
Tubulin alpha (Tba-2)	gi:17506073
ATP synthase a andb subunits (Vba-13)	gi:17565854
ATP synthase subunit 2 (Atp-2)	gi:25144756
Aconitate hydratase (Aco-1)	gi:17568399
Aconitase protein 2 isoform c (Aco-2)	gi:32564738
Aldo-keto reductase	gi:17564128
Transketolase	gi:17539652
Aldo-keto reductase family 1 member C1	gi:17550248
Protein disulfide isomerase 3 (Pdi-3)	gi:17507915
Stress-induced phosphoprotein 1-like	gi:17563052
Calreticulin (Crt-1)	gi:17565428
Chaperonin-containing TCP-1 (Cct-4)	gi:17532603
Aspartic protease precursor	gi:17560290
Aspartic protease 2 (Asp-2)	gi:32566657
Metalloenzyme	gi:32564249
14-3-3 protein 2 (Ftt-2)	gi:17568359
Galectin (Lec-6)	gi:17556226
Ribosomal protein small subunit (Rps-12)	gi:17554772
Nucleosome assembly 1-like (Nap-1)	gi:17539540

FIGURE 3. **Identification and validation of candidate CED-3 substrates.** *A*, proteins reproducibly altered upon treatment of *C. elegans* lysates with GST-CED-3 and identified by MALDI-TOF mass spectrometry (see supplemental Table S1 for full details). *B–D*, [^{35}S]methionine-labeled FTT-2 (*B*), CRT-1 (*C*), and TBB-2 (*D*) were incubated alongside pro-CED-3 and CED-9 with a range of concentrations of GST-CED-3 for 2 h at 37 °C. Ratios shown represent dilutions of the CED-3 protease stock. The stock concentration of CED-3 was 400 nM; therefore, the concentrations used were 100, 50, and 25 nM. The reaction products were resolved by SDS-PAGE. Cleavage site aspartates were then mutated to glutamates by site-directed mutagenesis. Mutant and wild type proteins were incubated with GST-CED-3 at 200, 100, 50, and 25 nM, and subjected to SDS-PAGE as above. Schematic representations of substrate proteins are shown below with CED-3 cleavage sites indicated.

CED-3-dependent Proteolysis in C. elegans Homogenates—To screen for CED-3 substrates within the *C. elegans* proteome, we generated worm homogenates as follows. Mixed stage populations of *C. elegans* were grown in liquid cultures until bacteria were entirely cleared because this facilitated the elimination of contaminating *E. coli* from the worm digestive tracts. Worms were then washed several times in M9 buffer followed by purification over sucrose gradients. Homogenates of worm populations were generated by brief sonication, and the resulting protein preparations were clarified by centrifugation at 15,000 × *g* to eliminate unbroken worms and empty cuticles (supplemental Fig. S3). These preparations were then incubated for 2 h at 37 °C in the presence or absence of recombinant CED-3. The concentration of CED-3 chosen was based upon preliminary titrations of recombinant CED-3 against known substrates, in the presence and absence of worm homogenates (as shown in Fig. 1*D*). Proteins were separated by one-dimensional SDS-PAGE. As shown in Fig. 2*A*, incubation of *C. elegans* homogenates with active GST-CED-3 failed to reveal any obvious alterations to the worm proteome, suggesting that CED-3 is a highly specific protease that cleaves relatively few substrate proteins, at least at concentrations where this protease can process its own precursor (Fig. 1*D*).

We next analyzed similar CED-3-treated worm homogenates using two-dimensional SDS-PAGE, and these analyses were successful in detecting ~40 alterations to the two-dimensional protein spot patterns (Fig. 2, *B* and *C*, and supplemental Fig. S4). Altered protein spots were then excised from the gels, and the proteins were identified by MALDI-TOF mass spectrometry. As illustrated in Fig. 3*A* and supplemental Table 1, 22 proteins were identified as undergoing CED-3-dependent proteolysis under these conditions. These included proteins involved in a diverse range of cellular functions. Of note, several homologues of known human caspase substrates were identified, including the cytoskeletal proteins actin, myosin, and α-tubulin (19, 20); a 14-3-3 protein (21); and a nucleosome assembly protein-1 homologue (22). Additionally, several of the substrates identified, including actin, myosin, tubulin, and calreticulin, have previously been implicated in apoptosis-associated events in mammalian systems (20, 23–25).

TABLE 1

Alignment of CED-3 cleavage sites

Sites of CED-3-mediated cleavage identified by site-directed mutagenesis in FTT-2, TBB-2, and CRT-1 were aligned with known CED-3 cleavage sites in CED-3 and CED-9. This alignment was used to derive a consensus sequence for CED-3-mediated protein cleavage motifs.

Substrate	Cleavage site				
	P4	P3	P2	P1	P1'
CED-3	N	F	V	D^{220}	A
	D	S	V	D^{374}	G
	D	N	R	D^{388}	G
CED-9	D	A	Q	D^{47}	L
	E	S	I	D^{67}	G
CRT-1	V	K	I	D^{182}	G
	D	A	E	D^{225}	A
	D	E	M	D^{253}	G
TBB-2	E	G	M	D^{404}	E
	N	M	N	D^{417}	L
	D	D	V	D^{435}	G
FTT-2	D	D	T	D^{240}	A
Consensus	**D**	**X**	**X**	**D**	**G**

Validation of CED-3 Substrates—To confirm that the identified proteins were *bona fide* CED-3 substrates rather than two-dimensional PAGE running artifacts, we cloned several of the genes encoding these proteins and explored whether *in vitro* transcribed and translated forms of these proteins were cleaved by CED-3 *in vitro*. As Fig. 3 (*B–D*) illustrates, 14-3-3 family protein 2 (FTT-2), calreticulin (CRT-1), and tubulin β2 (TBB-2) were cleaved by CED-3 with comparable efficiency to the known substrates pro-CED-3 and CED-9. In contrast, a panel of control worm proteins failed to undergo substantial proteolysis under the same conditions (supplemental Fig. S5).

Sites of CED-3-mediated cleavage in FTT-2, CRT-1, and TBB-2 were mapped by site-directed mutagenesis as shown in Fig. 3 (*B–D*). In the case of FTT-2, a single CED-3 cleavage site (Asp^{240}) appeared to be responsible for the proteolysis seen, because mutation of this site completely suppressed FTT-2 cleavage by CED-3 (Fig. 3*B*). In the case of TBB-2, mutation of three potential sites individually caused changes in the pattern of substrate proteolysis (data not shown), whereas mutation of all three sites simultaneously resulted in only a partial reduction in substrate cleavage efficiency, suggesting that multiple CED-3 cleavage sites are present in TBB-2 (Fig. 3*C*). A similar situation prevailed in the case of CRT-1, although mutation of three candidate sites in this protein did substantially attenuate proteolysis by CED-3 (Fig. 3*D*). The majority of the sites found in these substrates were found to match the consensus D*XX*D (Table 1), which is also typical of mammalian effector caspases. In addition, where multiple cleavage sites existed within a particular substrate, sites matching the D*XX*D consensus were the most efficiently cleaved (data not shown).

Cleavage of Human Homologues—Although it was not possible because of the lack of suitable antibodies to explore whether all CED-3 substrate homologues were also caspase substrates in man, we were able to confirm this in the case of FTT-2 homologues 14-3-3β, ε, and τ, TBB-2 homologue β-tubulin isoform 5, and CRT-1 homologue calreticulin. As shown in Fig. 4*A*, three human 14-3-3 isoforms underwent caspase-mediated proteolysis in a human cell-free system based on Jurkat cell-free extracts, whereas a fourth isoform, 14-3-3 ζ, remained uncleaved (data not shown). Human β-tubulin and calreticulin were also confirmed to be caspase substrates in apoptotic cell extracts (Fig. 4, *B* and *C*).

Calreticulin Is Cleaved during Apoptosis and Exposed on the Surface of Apoptotic Cells—The identification of the endoplasmic reticulum chaperone calreticulin as a caspase substrate was particularly interesting, because a recent report has shown that calreticulin is exposed on the cell surface during apoptosis (25). Cell surface-exposed calreticulin acts as a ligand for CD91 on phagocytes, leading to engulfment of the apoptotic cell (25). Thus, calreticulin appears to act as an inducible engulfment signal, the appearance of which on the cell surface may be controlled by caspases. To explore this possibility, we first assessed whether cleavage of calreticulin occurred in human CEM cells after exposure to a range of pro-apoptotic stimuli (actinomycin D, tosylphenylalanylchloromethane, and DCI). Proteolysis of calreticulin was indeed observed during apoptosis, although a relatively small proportion of the total cellular protein appeared to be cleaved in comparison with substrates such as XIAP and caspase-9 (Fig. 4*D*). Because the majority of calreticulin in healthy cells is contained within the endoplasmic reticulum, this protein is largely inaccessible to caspases, which may explain the inefficient proteolysis seen during apoptosis. In contrast, when *in vitro* transcribed and translated calreticulin was added to cell-free extracts, where this protein was not protected by endoplasmic reticulum, very robust proteolysis of calreticulin was observed (Fig. 4*C*).

We then explored whether surface exposure of calreticulin during apoptosis could be detected by immunostaining with an anti-calreticulin antibody, as recently reported (25). As Fig. 5*A* illustrates, whereas healthy CEM cells exhibited little surface immunoreactivity for calreticulin (Crt), this changed dramatically upon exposure to actinomycin D, DCI, or etoposide (VP-16), all of which promoted robust apoptosis under these conditions. Significantly, when these cells were treated with the caspase inhibitor z-VAD-fmk, surface exposure of calreticulin was profoundly inhibited (Fig. 5*B*). In addition, CEM cells stably expressing the apoptosis inhibitory protein Bcl-2 also failed to exhibit an increase in surface calreticulin upon exposure to actinomycin D (Fig. 5*C*). In contrast, surface expression of calreticulin was readily detected in wild type CEM cells under the same conditions (Fig. 5*C*). Thus, caspase activity appears to be essential for the cell surface exposure of calreticulin during apoptosis.

DISCUSSION

In this study, we have identified 22 novel substrates of the *C. elegans* caspase CED-3. Because only four CED-3 sub-

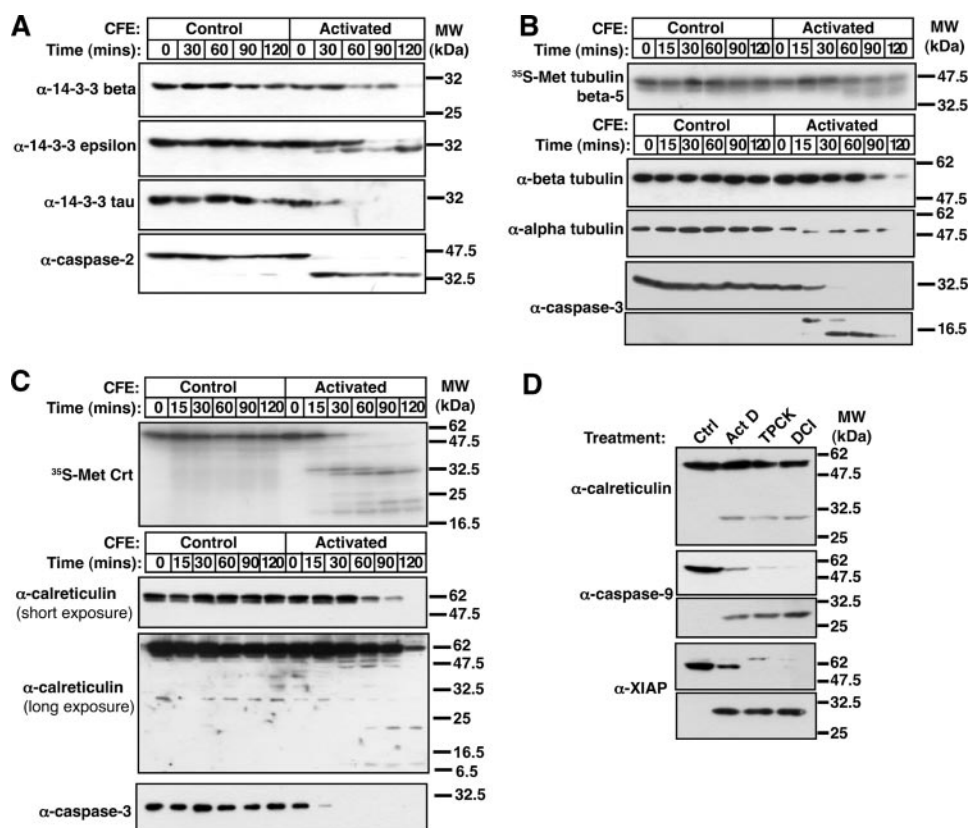## Identification of CED-3 Substrates

FIGURE 4. **Human homologues of CED-3 substrates are substrates for mammalian caspases.** *A*, human Jurkat cell extracts, untreated or treated with cytochrome *c* and dATP to activate caspases, were incubated at 37 °C for the indicated times. The samples were electrophoresed on 12% SDS-PAGE gels and analyzed by immunoblotting for isoforms of human 14-3-3 proteins and caspase-2. *B* and *C*, [^{35}S]methionine-labeled β-tubulin (*B*) and calreticulin (*C*) were incubated in Jurkat cell extracts treated as above for the indicated times, followed by electrophoresis on 12% SDS-PAGE gels. Extract samples were also analyzed by immunoblotting as above to detect β-tubulin, calreticulin (polyclonal antibody), and caspase-3. *D*, lysates were prepared from CEM cells treated for 12 h with the indicated drugs. The proteins were resolved by SDS-PAGE and substrate cleavage assessed by Western blotting (calreticulin monoclonal antibody). *CFE*, cell-free extract; *MW*, molecular mass.

strates have been identified to date (17, 18, 26), the present study represents a significant advance in our understanding of how CED-3 coordinates cell death. The substrates identified herein may be enriched in proteins that play important roles during CED-3-dependent cell death in the worm. Further analysis of the roles of these substrates may also yield novel insights into the execution phase of apoptosis in multiple organisms.

It is important to note that the approach we have used to identify CED-3 substrates has several potential drawbacks. First, because of the use of worm homogenates in our study, compartmentalization of many proteins will have been disrupted, and this may render such proteins more accessible to CED-3-mediated proteolysis than in intact cells. Second, we have used recombinant GST-CED-3 at concentrations that may well be significantly higher (or lower) than in worm cells undergoing programmed cell death. Because of the lack of suitable antibodies to measure this, the concentration of CED-3 expressed in worm cells undergoing PCD remains unknown. Third, the use of two-dimensional gels restricted us to visualizing only the most abundant proteins within the worm proteome. Thus, there is a high probability that numerous additional *C. elegans* proteins, of relatively low

abundance, are also subjected to proteolysis by CED-3 during cell death.

These caveats beg the question of why we pursued the biochemical approach adopted in this study, as opposed to analyzing CED-3-dependent proteolysis in dying worm cells for example? The answer to this is very straightforward. Because of the very small percentages (~12%) of cells undergoing developmental PCD in the worm, coupled with the fact that such cell deaths are asynchronous, it was technically unfeasible to detect CED-3-dependent changes to the worm proteome using intact worms or embryos (data not shown). Furthermore, as noted under "Results," numerous attempts to induce coordinate cell death in worm embryos or adults (using UV radiation, cancer chemotherapeutic drugs, protein and RNA synthesis inhibitors, and heat shock) were unsuccessful.[3] Indeed, it is likely that the combination of these factors have contributed to the remarkable paucity of knowledge concerning the mechanism of action of CED-3 during worm PCD.

CED-3 plays a dual role in worm PCD, acting as an initiator as well as an executioner caspase in this organism. We also explored the relationship of CED-3 to human caspase-3 in terms of substrate specificity. Using fluorogenic peptide substrates, CED-3 exhibited a clear preference for DEVD-AFC, reflecting its close relationship to the human executioner caspase-3. Indeed, the closest sequence homologues of CED-3 in humans are the executioner caspases caspase-3 and caspase-7. However, CED-3 exhibited a higher degree of promiscuity in its ability to hydrolyze the substrates IETD-AFC and LEHD-AFC, reflecting its broader role in *C. elegans* PCD. This preference was reflected in the CED-3 cleavage sites identified in protein substrates (Table 1). 7 of 12 known CED-3 cleavage sites match a D*XX*D consensus. Among the other sites, the P4 aspartate was substituted for glutamic acid (two sites), asparagine (two sites), or valine (one site). Where multiple sites were present, D*XX*D sites were the most readily cleaved (data not shown). Interestingly, the P1′ site was in all but one case occupied by a small amino acid, suggesting that CED-3 cleavage site specificity may extend further than the traditional tetrapeptide motif, as suggested for several of the human caspases (27).

During the execution phase of apoptosis, cells undergo a stereotypical set of morphological changes including detachment and rounding, membrane blebbing, fragmenta-
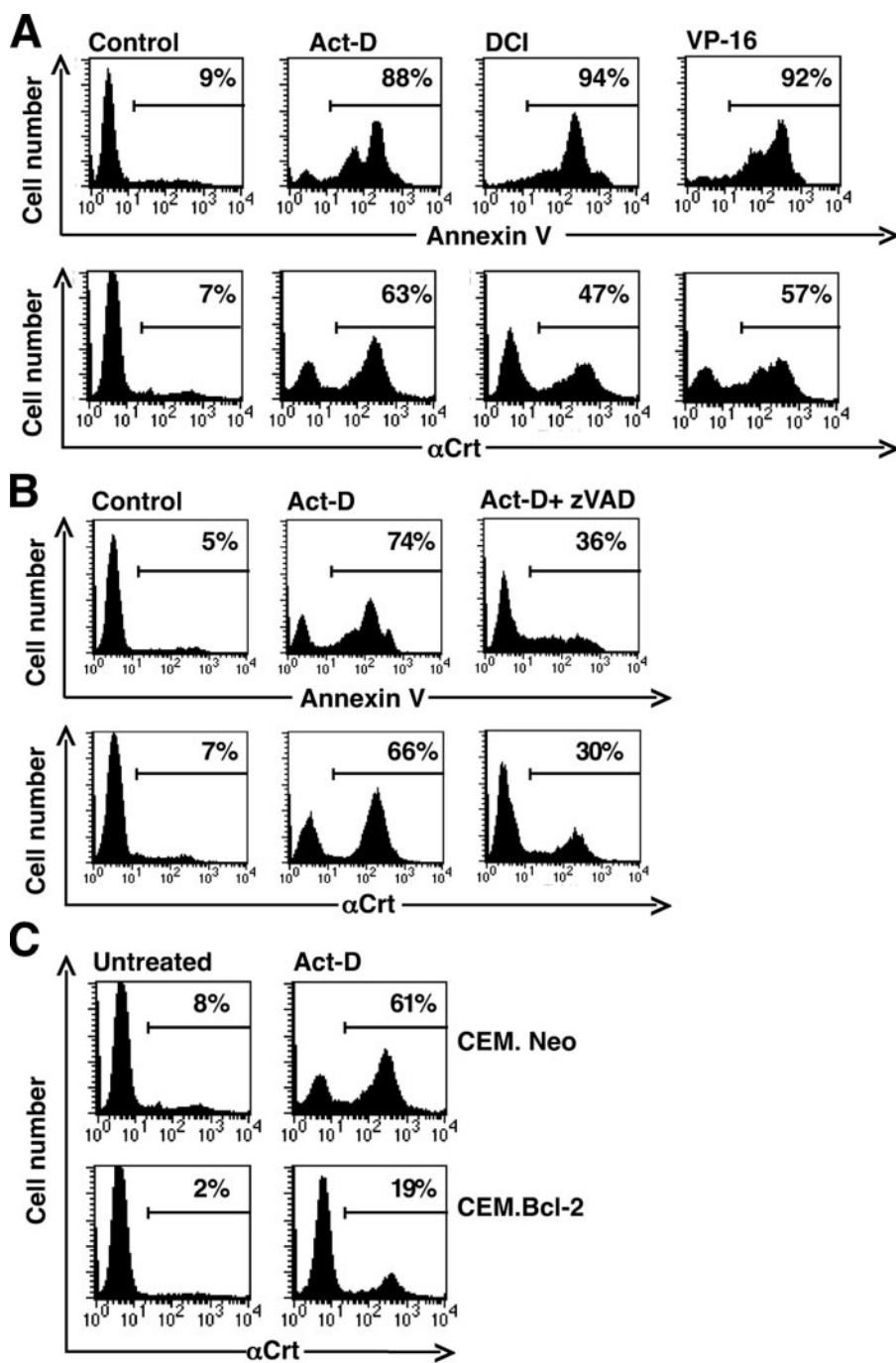
FIGURE 5. **Exposure of calreticulin on the dying cell surface is dependent upon caspase activity.** *A*, CEM cells were treated with actinomycin D (*Act-D*, 20 μM), DCI (100 μM), or VP-16 (100 μM) followed by staining with annexin V or immunostaining with anti-calreticulin antibodies. Representative FACS plots are shown. *B*, CEM.neo cells were incubated for 12 h in the presence of 20 μM actinomycin D with or without 50 μM z-VAD-fmk, followed by staining with annexin V and surface immunostaining with anti-calreticulin. Representative FACS plots are shown. *C*, CEM.neo and CEM.Bcl-2 cells were incubated with 20 μM actinomycin D for 12 h followed by surface immunostaining with anti-calreticulin. Representative FACS plots are shown.

force for cell blebbing and fragmentation (23, 24, 28), whereas changes in microtubules may act to transport fragmented chromatin or phagocytic effectors into late stage blebs (29). Because removal of the C terminus of human α-tubulin by the serine protease granzyme B results in increased rates of polymerization (20), it may be that removal of tubulin C termini by proteases is a common mechanism of functional disruption of microtubules during apoptosis.

Changes in apoptotic cells require energy, and during early stages of apoptosis ATP generation systems remain unperturbed. However, later stages of apoptosis are characterized by a shutdown of energy production, and cleavage of ATP synthase subunits may contribute to this. Interestingly, the vacuolar ATP synthase of which VBA-13 is a subunit has been recently implicated in generating the acidic conditions required for neurodegeneration (30). This suggests that disabling the vacuolar ATPase may prevent dying cells from undergoing necrosis before completion of the PCD pathway. In addition, many substrates identified here are involved in cellular metabolism. This may reflect a general shutdown of energy-consuming processes in apoptotic cells. It may also help to ensure the irreversibility of the apoptotic process, because cells are unable to survive once essential processes are shut down. However, the abundance of metabolic proteins identified in this analysis is possibly due to the proteomics technology used because two-dimensional electrophoresis reveals the most abundant proteins within the proteome, among which proteins with metabolic functions are over-represented.

Other cleavage events may function to disable cell survival pathways. 14-3-3 proteins such as FTT-2 play roles in several survival pathways and have already been identified as substrates of human caspases (21). Chaperone proteins may also be targeted during apoptosis to prevent futile attempts to prolong survival. Interestingly, the chaperone substrate calreticulin is required for necrosis in *C. elegans* (31). Recent

tion of chromatin and cellular organelles, formation of apoptotic bodies, and the exposure of "eat me" signals for phagocytes. In keeping with this, proteins targeted by CED-3 are involved in diverse cellular functions. Notably, several are components of the cytoskeleton, and these substrates already have known roles in apoptosis-associated events. Actin and myosin are thought to provide the contractile

studies also suggests that calreticulin is exposed on the cell surface during apoptosis and acts as a signal allowing phagocyte attachment and cell engulfment (25, 32). Furthermore, caspase-dependent exposure of calreticulin in response to certain pro-apoptotic stimuli appears to influence the immunogenicity of tumors (32). Thus, dying cells with elevated levels of surface calreticulin provoked strong immune-mediated clearance that may be related to the efficiency of uptake of the latter cells by dentritic cells (32). Here we have provided evidence that cleavage of calreticulin by caspases influences its surface exposure by a mechanism that remains to be defined.

Another intriguing observation was the identification of two aspartic proteases as CED-3 substrates. This raises the possibility that a protease activation cascade exists in the worm, involving aspartic as well as caspase proteases. In mammalian systems, it has frequently been suggested that proteases other than caspases may play a role in cell death. This leaves open the possibility that some of the proteins altered in our analysis may in fact be targets of these other proteases and are therefore indirect results of CED-3 activation. Alternatively, because these aspartic proteases are related to proteases implicated in necrotic cell death in *C. elegans* (33), cleavage by CED-3 might inactivate such proteases to ensure that cells undergoing PCD do not manifest necrotic changes. The observation that 4 of the 22 substrates identified here are potentially required for necrosis in *C. elegans* may reflect a general strategy to prevent diversion of apoptotic cells into necrosis.

Although few substrates for CED-3 have previously been described, almost 400 substrates for the mammalian caspases have now been identified (34). However, the vast majority of these substrates have been identified, at random, over a period of 10 years or so. Few systematic searches for caspase substrates, similar to the one reported here, have been conducted to date. One recent study used a non-gel chromatography-based approach, coupled with mass spectrometry, to search for human caspase substrates in Jurkat cells undergoing apoptosis in response to CD95 receptor ligation (22). This approach yielded 92 putative caspase substrates, some of which were validated as *bona fide* substrates for these proteases. The latter study adopted a novel and sensitive method for the detection of newly generated protein N termini (22). However, even with sophisticated methods such as those employed by Van Damme *et al.* (22), it is clear that proteomics-based screening approaches do not completely cover the proteome, because several hundred known caspase substrates were not detected by this approach (34). Clearly, several factors can influence the likelihood of detecting proteolysis of particular proteins, including the source of the tissue used for the analysis (which will have an impact on the relative abundance of particular proteins), the analytical method employed (*e.g.* some proteins resolve very poorly on two-dimensional gels because of size and charge issues, some peptides do not fly well in mass spectrometers), the efficiency of proteolysis of particular substrates, and other factors. Because of the above consider-

ations, it is highly likely that many more substrates for CED-3 will be found by using complementary approaches.

In summary, this study provides the first detailed analysis of the proteins that undergo CED-3-dependent proteolysis in the nematode *C. elegans* and reveals that CED-3 targets a relatively restricted set of proteins to coordinate cell death, many of which are conserved caspase substrates in mammals.

REFERENCES

1. Earnshaw, W. C., Martins, L. M., and Kaufmann, S. H. (1999) *Annu. Rev. Biochem.* **68,** 383–424
2. Martin, S. J., and Green, D. R. (1995) *Cell* **82,** 349–352
3. Stennicke, H. R., and Salvesen, G. S. (1999) *Cell Death Differ.* **6,** 1054–1059
4. Fischer, U., Janicke, R. U., and Schulze-Osthoff, K. (2003) *Cell Death Differ.* **10,** 76–100
5. Savill, J., and Fadok, V. (2000) *Nature* **407,** 784–788
6. Ellis, R. E., and Horvitz, H. R. (1986) *Cell* **44,** 817–829
7. Lettre, G., and Hengartner, M. O. (2006) *Nat. Rev. Mol. Cell. Biol.* **7,** 97–108
8. Yuan, J., Shaham, S., Ledoux, S., Ellis, H. M., and Horvitz, H. R. (1993) *Cell* **75,** 641–652
9. Miura, M., Zhu, H., Rotello, R., Hartwieg, E. A., and Yuan, J. (1993) *Cell* **175,** 653–660
10. Nicholson, D. W., Ali, A., Thornberry, N. A., Vaillancourt, J. P., Ding, C. K., Gallant, M., Gareau, Y., Griffin, P. R., Labelle, M., Lazebnik, Y. A., Munday, N. A., Raju, S. M., Smulson, M. E., Yamin, T. T., Yu, V. L., and Miller, D. K. (1995) *Nature* **376,** 37–43
11. Shaham, S., Reddien, P. W., Davies, B., and Horvitz, H. R. (1999) *Genetics* **153,** 1655–1671
12. Yan, N., Chai, J., Lee, E. S., Gu, L., Liu, Q., He, J., Wu, J. W., Kokel, D., Li, H., Hao, Q., Xue, D., and Shi, Y. (2005) *Nature* **437,** 831–837
13. Hengartner, M. O., Ellis, R. E., and Horvitz, H. R. (1992) *Nature* **356,** 494–499
14. Adrain, C., Creagh, E. M., Cullen, S. P., and Martin, S. J. (2004) *J. Biol. Chem.* **279,** 36923–36930
15. Slee, E. A., Harte, M. T., Kluck, R. M., Wolf, B. B., Casiano, C. A., Newmeyer, D. D., Wang, H. G., Reed, J. C., Nicholson, D. W., Alnemri, E. S., Green, D. R., and Martin, S. J. (1999) *J. Cell Biol.* **144,** 281–292
16. Sulston, J. E., and Horvitz, H. R. (1977) *Dev. Biol.* **56,** 110–156
17. Xue, D., Shaham, S., and Horvitz, H. R. (1996) *Genes Dev.* **10,** 1073–1083
18. Xue, D., and Horvitz, H. R. (1997) *Nature* **390,** 305–308
19. Moretti, A., Weig, H. J., Ott, T., Seyfarth, M., Holthoff, H. P., Grewe, D., Gillitzer, A., Bott-Flugel, L., Schomig, A., Ungerer, M., and Laugwitz, K. L. (2002) *Proc. Natl. Acad. Sci. U. S. A.* **99,** 11860–11865
20. Adrain, C., Duriez, P. J., Brumatti, G., Delivani, P., and Martin, S. J. (2006) *J. Biol. Chem.* **281,** 38118–38125
21. Won, J., Kim, D. Y., La, M., Kim, D., Meadows, G. G., and Joe, C. O. (2003) *J. Biol. Chem.* **278,** 19347–19351
22. Van Damme, P., Martens, L., Van Damme, J., Hugelier, K., Staes, A., Vandekerckhove, J., and Gevaert, K. (2005) *Nat. Methods* **2,** 771–777
23. Coleman, M. L., Sahai, E. A., Yeo, M., Bosch, M., Dewar, A., and Olson, M. F. (2001) *Nat. Cell Biol.* **3,** 339–345
24. Sebbagh, M., Renvoize, C., Hamelin, J., Riche, N., Bertoglio, J., and Breard, J. (2001) *Nat. Cell Biol.* **3,** 346–532
25. Gardai, S. J., McPhillips, K. A., Frasch, S. C., Janssen, W. J., Starefeldt, A., Murphy-Ullrich, J. E., Bratton, D. L., Oldenborg, P., Michalak, M., and Henson, P. M. (2005) *Cell* **123,** 321–334
26. Kim, S. Y., Valencia, M., Lee, E. S., Park, D., Oh, M., Xue, D., and Park, W. J. (2004) *Mol. Biotechnol.* **27,** 1–6
27. Stennicke, H. R., Renatus, M., Meldal, M., and Salvesen, G. S. (2000) *Bio-*

chem. J. **350,** 563–568

28. Mills, J. C., Stone, N. L., Erhardt, J., and Pittman, R. N. (1998) *J. Cell Biol.* **140,** 627–636
29. Moss, D. K., Betin, V. M., Malesinski, S. D., and Lane, J. D. (2006) *J. Cell Sci.* **119,** 2362–2374
30. Syntichaki, P., Samara, C., and Tavernarakis, N. (2005) *Curr. Biol.* **15,** 1249–1254
31. Xu, K., Tavernarakis, N., and Driscoll, M. (2001) *Neuron* **31,** 957–971
32. Obeid, M., Tesniere, A., Ghiringhelli, F., Fimia, G. M., Apetoh, L., Perfet-tini, J. L., Castedo, M., Mignot, G., Panaretakis, T., Casares, N., Metivier, D., Larochette, N., van Endert, P., Ciccosanti, F., Piacentini, M., Zitvogel, L., and Kroemer, G. (2007) *Nat. Med.* **13,** 54–61
33. Syntichaki, P., Xu, K., Driscoll, M., and Tavernarakis, N. (2002) *Nature* **419,** 939–944
34. Luthi, A. U., and Martin S. J. (2007) *Cell Death Differ.* **14,** 641–650
35. Martin, S. J., Amarante-Mendes, G. P., Shi, L., Chuang, T. H., Casiano, C. A., O'Brien, G. A., Fitzgerald, P., Tan, E. M., Bokoch, G. M., Greenberg, A. H., and Green, D. R. (1996) *EMBO J.* **15,** 2407–2416

Molecular Basis of Cell and
Developmental Biology:
**Establishing a Blueprint for
CED-3-dependent Killing through
Identification of Multiple Substrates for
This Protease**

Rebecca C. Taylor, Gabriela Brumatti, Shu
Ito, Michael O. Hengartner, W. Brent Derry
and Seamus J. Martin

Access the most updated version of this article at doi: 10.1074/jbc.M611051200

Find articles, minireviews, Reflections and Classics on similar topics on the JBC Affinity Sites.

Alerts:
- When this article is cited
- When a correction for this article is posted

Click here to choose from all of JBC's e-mail alerts

Supplemental material:
http://www.jbc.org/content/suppl/2007/03/19/M611051200.DC1.html

This article cites 35 references, 9 of which can be accessed free at
http://www.jbc.org/content/282/20/15011.full.html#ref-list-1